electronic reprint

Journal of
Applied Crystallography
ISSN 0021-8898

The development and application of a method to quantify the quality of cryoprotectant solutions using standard area-detector X-ray images

Michael B. McFerrin and Edward H. Snell

Journal of
Applied Crystallography
ISSN 0021-8898

Received 21 March 2002
Accepted 21 May 2002

The development and application of a method to quantify the quality of cryoprotectant solutions using standard area-detector X-ray images

Michael B. McFerrin and Edward H. Snell*

NASA Laboratory for Structural Biology, Code SD46, MSFC, Huntsville, AL 35812, USA.
Correspondence e-mail: eddie.snell@msfc.nasa.gov

An X-ray based method for determining initial cryoprotectant concentrations necessary to protect solutions from crystalline ice formation on flash cooling was developed. X-ray images from a charge-coupled device (CCD) area detector were integrated as powder patterns and quantified by determining the standard deviation of the slope of the normalized intensity curve in the resolution range where ice rings are known to occur. The method was tested by determining the concentrations of glycerol, PEG400, ethylene glycol and 1,2-propanediol necessary to form an amorphous glass at 100 K with each of the 98 crystallization solutions of Crystal Screens I and II (Hampton Research, Laguna Hills, California, USA). For conditions that required glycerol concentrations of 35% or above, cryoprotectant conditions using (2*R*,3*R*)-(−)-2,3-butanediol were determined. The method proved to be remarkably reliable. The results build on previous work [Garman & Mitchell (1996). *J. Appl. Cryst.* **29**, 584–587] and extend the number of suitable starting conditions to alternative cryoprotectants.

1. Introduction

Macromolecular crystal X-ray data collection at cryogenic temperatures (∼100 K) has become routine in the home laboratory and is especially important at synchrotron sources. Cryoprotection of crystals greatly reduces radiation damage from the X-ray beam and improves data quality as a result of reduced thermal motion (atomic displacement factors). This has enhanced many studies, such as ultra-high resolution data collection and MAD phasing methods. Cryogenic techniques have been well reviewed (Garman, 1999; Garman & Schneider, 1997; Rodgers, 1994, 1997). The key to the technique is preventing ice crystal nucleation by forming an amorphous glass upon cooling of the sample. Typically cryoprotectants are added that impede nucleation and growth of ice crystals, thus enabling glass formation (Angell & Choi, 1986; Echlin, 1992; Steinbrecht & Zierold, 1987).

Several commonly used cryoprotectants include glycerol, ethylene glycol, MPD, PEGs, sucrose, erythritol and xylitol. Garman & Mitchell (1996) published the glycerol concentrations required to form an amorphous glass during cryocooling of the 50 Hampton Research Crystal Screen I solutions (Jancarik & Kim, 1991). In that study, X-ray images were collected for 5% increments in glycerol concentration until ice rings vanished and a cross section through the diffuse scattering ring had similar slopes on both the high- and the low-resolution side. We have developed a quantitative analysis technique and used it here to expand the work of Garman & Mitchell (1996). A further 48 cryoprotectant conditions with glycerol and 98 conditions of the Hampton Screens I and II with PEG400, ethylene glycol and 1,2-propanediol have been determined using the method.

2. Experimental

A video microscope system was set up off-line consisting of a COHU CCD, NAVITAR optical telescope, front and side illumination, and a Bandit frame grabber board. The system was focused on an alignment pin positioned on a rotatable goniometer illuminated from both front and back. An Oxford 600 Cryostream (Cosier & Glazer, 1986) was positioned such that its tip was 5 mm from the alignment pin at an angle of 45°. The cryostream was operated at 100 K and the alignment pin replaced with a magnetic mount. The goniometer head was translated vertically such that the cryoloops used in the experiment were in the center of the field of view when mounted on the magnetic mount.

Using a similar method to that of Garman & Mitchell (1996), glycerol was heated in a water bath to 343 K and measured out in 30 µl quantities using a positive displacement pipette into 600 µL microfuge tubes. Heating the glycerol reduced its viscosity and so allowed accurate repeated dispensing of the required volume. Six Hampton Screen I solutions, conditions 2, 6, 33, 36, 38 and 47, were used sequentially to make up concentrations with cryoprotectant increasing in 5% increments. These conditions were chosen to represent a sample of the conditions originally described by Garman & Mitchell (1996). Testing these conditions was carried out to ensure our results and methodologies were

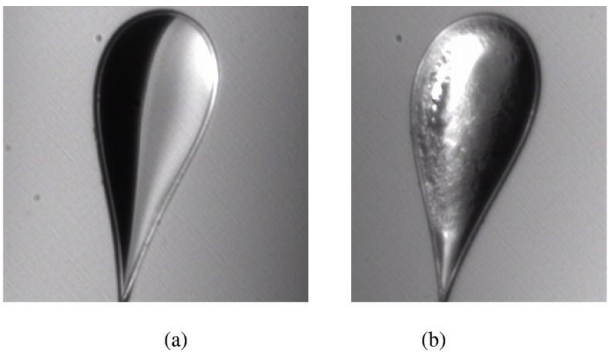

Figure 1
Digital video microscope image showing (*a*) a clear drop indicating a visually successful cryoprotectant condition and (*b*) a failure, an opaque drop with surface ice features.

comparable with those of Garman & Mitchell. A 20 μm nylon cryoloop of diameter 0.7–1.0 mm was used to pick up a sample of the cryoprotected solution, with the loop nearly parallel to the surface of the solution, and position it on the goniometer head in the cryostream. The video microscope provided a clear image of the loop in the 100 K nitrogen gas stream. Successful cryocooling was defined as that which gave a transparent smooth glass in the loop under ideal illumination (Fig. 1*a*). The sample was warmed and allowed to recool to ensure the conditions formed a smooth transparent glass repeatedly. An unsuccessful cryocooling attempt was defined as one that had any evidence of opaqueness, features such as lines, or clear ice formation, *e.g.* Fig. 1(*b*). In the event of an unsuccessful cooling attempt, the glycerol concentration was increased by 5% and the experiment repeated. A similar procedure was repeated for glycerol with each of the conditions in Hampton Screen II.

The percentage of glycerol found from visual observation of successful cooling was used as a starting point for X-ray analysis. X-ray data were collected using a Nonius Kappa2000 CCD detector and an FR591 rotating anode source. A similar cryostat arrangement was used as in the off-line experiments, with an Oxford 600 Cryostream, operating at 100 K, an angle of incidence of 45° and a distance of 5 mm from the end of the nozzle to the sample loop. X-ray images were taken at 5% below the concentration percentage that had been visually determined to be successful. Successive images were taken at 5% intervals until no features were seen in the diffraction pattern. If the lowest-concentration image did not show clear rings (ice or strong diffuse scatter) images were recorded in decreasing steps of 5% until rings were seen. The X-ray generator operated at 47 kV and 100 mA with a 0.3 mm diameter collimator and a sample to detector distance of 75 mm, giving a resolution of 2.8 Å at the edge and 2.3 Å at the corners of the detector. The exposure time of 15 s was determined by imaging of several imperfect conditions showing opaqueness or ice in the video microscope images. These conditions clearly showed diffraction features in this exposure time. The loop was positioned such that it was perpendicular to the X-ray beam. An image of a blank loop perpendicular to the beam was taken as a reference image and an image of the loop parallel to the beam was recorded for comparison.

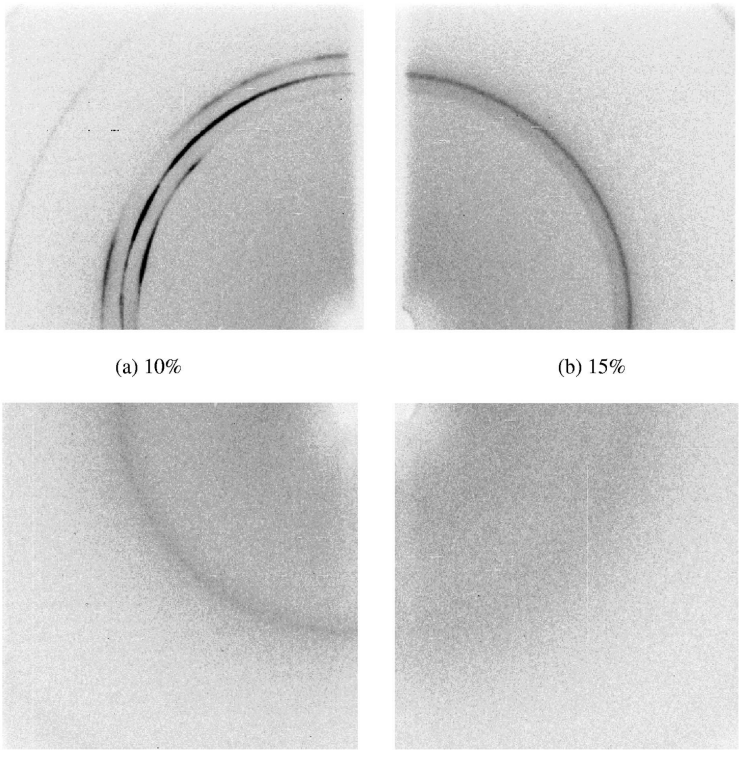

Figure 2
X-ray images of Hampton Screen II condition 22, 0.1 *M* MES pH 6.5, 12% *w*/*v* PEG 20000, showing one quarter of the imaged area for (*a*) 10%, (*b*) 15%, (*c*) 20% and (*d*) 25% 1,2-propanediol.

Each X-ray image was visually examined. It was then integrated as a powder diffraction pattern using the *POWDERIZE* program of the Nonius *COLLECT* data processing software. A least-squares fit line was determined based on the regions of data that represented background scatter, where the peaks resulting from ice formation were not observed (from 7 to 17°, and 31 to 40° in 2θ; 12.7 to 5.3 Å, and 3.0 to 2.4 Å resolution). The reference image of the blank loop was then treated in the same manner to establish a trend-line for the basal level of background scatter. The trend-line from the sample data was then divided by the blank-loop trend-line to produce a scale factor for each point in the sample data. The sample data were then divided by this scale factor at each point, effectively normalizing the data to that of the blank loop. An approximation of the derivative was taken at each point of the sample data. The derivative was very sensitive to changes in intensity caused by ice rings. To reduce noise, the standard deviation of the derivative was determined for the 'signal' region of the data (between 17 and 31° in 2θ; between 5.3 and 3.0 Å resolution). This standard deviation value was used as a quantitative measure of the quality of the cryo-

cooling. A higher standard deviation indicated significant variation of intensity with 2θ, as seen in the case of sharp ice rings in the image, as shown in Fig. 2(*a*). As the cryoprotectant percentage increases, the glass/crystalline ice ratio increases and the ice rings change from sharp to diffuse in nature, as shown in Fig. 2, reducing the intensity variation and, hence, decreasing the standard deviation of the derivative of the intensity. The maximum value of the standard deviation below which good cryoprotectant conditions were obtained for X-ray data collection was empirically determined to be 1.5.

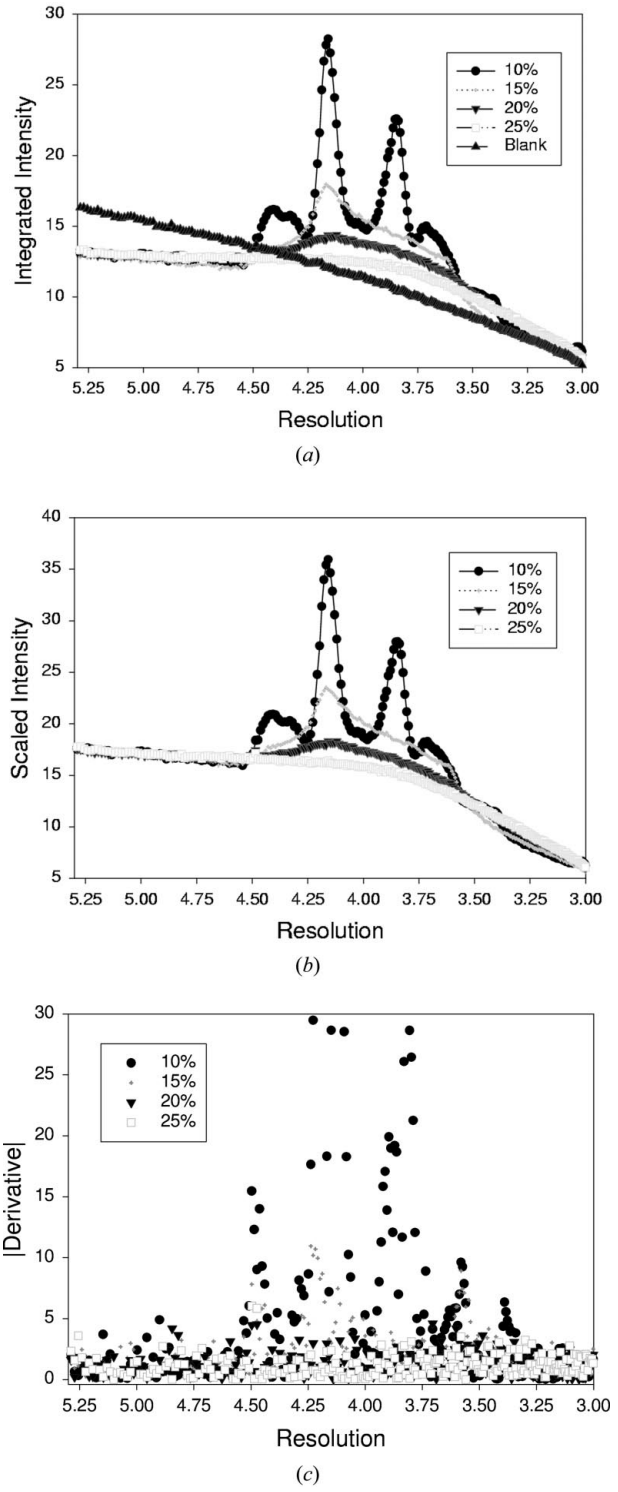

Figure 3
(*a*) The powder integrated intensity, (*b*) the normalized data and (*c*) the differential for the X-ray images in Fig. 2 of Hampton Screen II, condition 22 and different percentages of 1,2-propanediol.

A similar treatment was extended to the PEG400, ethylene glycol and 1,2-propanediol cryoprotectants for both the Hampton Screens, I and II. For those conditions that required a glycerol concentration of 35% or greater, the percentage of (2*R*,3*R*)-(−)-2,3-butanediol necessary to form an amorphous glass was determined in a like manner. The cryoprotectant (2*R*,3*R*)-(−)-2,3-butanediol is significantly more expensive than the other cryoprotectants used in the study, but not prohibitively so given the small quantities needed. It should be noted that the cryoprotectant solutions in this study were made such that the crystal screen solution was diluted with the cryoprotecting agent. Ideally, the cryoprotectant would replace the water in the crystallization solution. Additionally, MPD and xylitol were explored as possible cryoprotectants for these 98 crystallization solutions. It soon became evident that MPD and xylitol required much higher concentrations to become visually clear and X-ray analysis was not carried out on these samples. Finally, water was analyzed with the addition of increasing concentrations of the cryoprotectants.

The amount of cryoprotectant present in the loops was measured to give an indication of differences in the volumes arising from different viscosity/surface-tension effects. The loop used to obtain X-ray data from the various cryosolutions was weighed on an analytical balance (sensitive to 0.01 mg). Then the loop was dipped into 100% cryoprotectant, a sample obtained with the plane of the loop nearly parallel to the surface of the cryoprotectant, and the loop plus sample weighed. The weight of the cryoprotectant in the loop was determined and the volume calculated from the density of the liquid at room temperature as reported in the literature. This was repeated five times for each cryoprotectant and the results averaged. The loop was rinsed with ethanol and allowed to dry thoroughly between weighing each sample.

To test the method as a possible automated diagnostic tool for detecting cooling problems during data collection, diffraction images were first collected from a cryocooled lysozyme crystal grown in the presence of 25% (*v*/*v*) ethylene glycol. Data were collected using a Kappa2000 CCD on a Nonius FR591 rotating anode running at 47 kV, 120 mA, with Osmic blue optics. A total of 60, 1° φ oscillation images were taken with the crystal at 100 K with an exposure time of 30 s per ° at $2\theta = 0°$, and a crystal to detector distance of 50 mm. The experiment was repeated using the same crystal and original starting position but with the cryostream programmed to warm up at a rate of 1 K min^{-1}, *i.e.* effectively 1 K per image. A total of 90 images were collected for this data set. The data sets were processed identically, integrating and scaling with *HKL2000* (Otwinowski & Minor, 1997). Each image was observed visually, integrated as a powder pattern, and analyzed in a similar way to the X-ray images obtained from the solutions.

Table 1
Standard deviation values (the cryoprotectant solution quality number) for 100% cryoprotectant and the average standard deviation obtained for the percentage of cryoprotectant necessary to protect successfully solutions from Hampton Screen I and II.

The average volume of cryoprotectant in the loop is listed. In the case of the average values, the standard deviation within those values is given in parentheses. Also shown are the maximum acceptable values (showing no visible ice rings) and the number that were greater than the sum of the average and standard deviation. For Hampton Screen I, only six conditions were tested with glycerol to verify the results of Garman & Mitchell (1996). Only the eight conditions requiring the highest percentage of glycerol were studied with (2*R*,3*R*)-(−)-2,3-butanediol. For reference, the standard deviation value for the empty loop was 0.74.

	Glycerol	PEG 400	Ethylene glycol	1,2-Propanediol	(2*R*,3*R*)-(−)-2,3-Butanediol
Volume in loop (µl)	0.12 (2)	0.09 (1)	0.06 (1)	0.06 (1)	0.12 (2)
Cryoprotectant quality index					
100% cryoprotectant solutions	1.74	2.16	2.57	2.21	1.001
Hampton Screen I					
Average standard deviation	1.01 (11)	1.09 (15)	1.10 (16)	1.37 (21)	1.21 (11)
Maximum	1.14	1.69	1.65	2.0	1.304
Greater than one standard deviation	17% (1/6)	8% (3/38)	12% (5/43)	19% (8/43)	0% (0/4)
Hampton Screen II					
Average	1.02 (19)	0.99 (15)	1.05 (14)	1.29 (11)	1.10 (07)
Maximum	1.56	1.38	1.42	1.64	1.19
Greater than one standard deviation	17% (7/41)	15% (5/33)	10% (4/41)	17% (7/41)	25% (1/4)

3. Results

To a first approximation, viewing the clearness of the solution upon flash cooling, with the illumination employed, was adequate to detect a cryosolution that did not produce ice rings when the subsequent X-ray data were examined. Viewing the X-ray data was subjective when trying to determine if one percentage concentration of cryoprotectant was better than another. Fig. 2 shows cryocooling of Hampton Screen II, condition 22, with 10, 15, 20 and finally 25% 1,2-pentanediol. As the cryoprotectant concentration is increased, there is a reduction of the intensity of ice rings present at 10%, which have become diffuse at a concentration of 20%, and are subsequently eliminated at a concentration of 25% cryoprotectant. The protocol used to analyze these images is illustrated in Fig. 3. The raw data are shown in Fig. 3(*a*) and in normalized form in Fig. 3(*b*). The derivative of these data is plotted in Fig. 3(*c*). The standard deviation values for the derivatives at 10, 15, 20 and 25% concentration of cryoprotectant are 11.80, 2.80, 1.42 and 1.20, respectively. We term this standard deviation value the cryoprotection quality index.

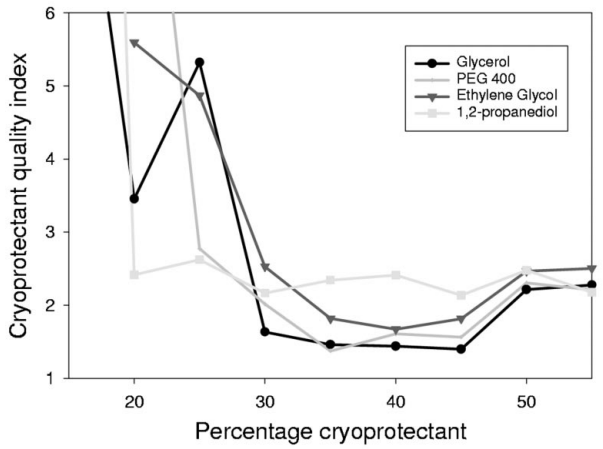

Figure 4
Cryoprotectant quality index as a function of cryoprotectant concentration in water.

Table 1 lists the standard deviations of the derivative values obtained for 100% solutions of the various cryoprotectants vitrified in the loop and the average values for successful cryocooling of the Hampton Screen solutions. The standard deviation for successful cryocooling conditions averaged to 1.12. The cryoprotectants themselves contribute differently to the measured signal. Ethylene glycol contributes the most signal, followed by PEG 400, 1,2-propanediol, glycerol and finally (2*R*,3*R*)-(−)-2,3-butanediol. Also shown in Table 1 is the volume of cryoprotectant in the loop. The volume of water in the loop, based on weight, was 0.19 (6) µl. There was more variability in the volume of water picked up in the loop than for the cryoprotectants. The differences seen in the intensity of X-ray scattering from the pure cryoprotectants do not seem to be related to the volume in the drop.

The results presented in Table 2 show the percentage of cryoprotectant needed to cryoprotect all 98 solutions from the two Hampton Screens. These were verified from the diffraction images, both visually and by the cryoprotectant quality number being less than or equal to 1.5. Solutions containing 30% MPD or more did not require additional cryoprotectant; solutions containing 30% PEG 400 in combination with at least 0.2 *M* salt also did not require cryoprotectant. These conditions seem to be borderline, as observed by Garman & Mitchell (1996). When PEG 400 is lowered to 28% in the case of Crystal Screen I, condition 14 (I-14), a minimal amount of cryoprotectant is needed. In the same manner, when the salt concentration is reduced to 0.1 *M*, as in Crystal Screen II, condition 12 (II-12), a minimal concentration of cryoprotectant is necessary for successful cryocooling. Similarly, 30% Jeffamine M-600 (II-24) required no additional cryoprotectant as this compound is a substituted polymer of poly-

Table 2
List of Hampton Screen I and II conditions and the percentage of cryoprotectant necessary for effective cryoprotection determined by X-ray data.

EG = ethyleneglycol; PG = propylene glycol (1,2-propanediol). Percentages in parentheses represent unsuccessful trials and are the percentage of cryoprotectant when the observed phenomenon took place. Six conditions listed in the text and indicated in bold in the table were experimentally determined with glycerol and Hampton Screen I. These agreed with the valus of Garman & Mitchell (1996). For the other 44 glycerol conditions and solutions of Hampton Screen I, the values of Garman & Mitchell (1996) are quoted.

(*a*) Hampton Screen I

#	Salt	Buffer	Precipitant	Glycerol	PEG 400	EG	PG
1	0.02 *M* Calcium Chloride	0.1 *M* Na Acetate pH 4.6	30% *v/v* MPD	None	None	None	None
2	None	None	0.4 *M* K/Na Tartrate	**35% *v/v***	30% *v/v*	30% *v/v*	25% *v/v*
3	None	None	0.4 *M* Ammonium Phosphate	35% *v/v*	35% *v/v*	35% *v/v*	30% *v/v*
4	None	0.1 *M* Tris HCl pH 8.5	2.0 *M* Ammonium Sulfate	25% *v/v*	15% *v/v*	25% *v/v*	20% *v/v*
5	0.2 *M* Na Citrate	0.1 *M* Na HEPES pH 7.5	30% *v/v* MPD	None	None	None	None
6	0.2 *M* Magnesium Chloride	0.1 *M* Tris HCl pH 8.5	30% *w/v* PEG 4000	**20% *v/v***	10% *v/v*	10% *v/v*	5% *v/v*
7	None	0.1 *M* Na Cacodylate pH 6.5	1.4 *M* Na Acetate	30% *v/v*	20% *v/v*	20% *v/v*	15% *v/v*
8	0.2 *M* Na Citrate	0.1 *M* Na Cacodylate pH 6.5	30% *v/v* Isopropanol	30% *v/v*	20% *v/v*	20% *v/v*	20% *v/v*
9	0.2 *M* Ammonium Acetate	0.1 *M* Na Citrate pH 5.6	30% *v/v* PEG 4000	15% *v/v*	5% *v/v*	10% *v/v*	5% *v/v*
10	0.2 *M* Ammonium Acetate	0.1 *M* Na Acetate pH 4.6	30% *v/v* PEG 4000	15% *v/v*	10% *v/v*	10% *v/v*	5% *v/v*
11	None	0.1 *M* Na Citrate pH 5.6	1.0 *M* Ammonium Phosphate	30% *v/v*	30% *v/v*	20% *v/v*	20% *v/v*
12	0.2 *M* Magnesium Chloride	0.1 *M* Na HEPES pH 7.5	30% *v/v* Isopropanol	10% *v/v*	25% *v/v*	20% *v/v*	10% *v/v*
13	0.2 *M* Na Citrate	0.1 *M* Tris HCl pH 8.5	30% *v/v* PEG 400	None	None	None	None
14	0.2 *M* Calcium Chloride	0.1 *M* Na HEPES pH 7.5	28% *v/v* PEG 400	5% *v/v*	5% *v/v*	10% *v/v*	5% *v/v*
15	0.2 *M* Ammonium Sulfate	0.1 *M* Na Cacodylate pH 6.5	30% *w/v* PEG 8000	15% *v/v*	10% *v/v*	10% *v/v*	5% *v/v*
16	None	0.1 *M* Na HEPES pH 7.5	1.5 *M* Lithium Sulfate	25% *v/v*	15% *v/v*	20% *v/v*	10% *v/v*
17	0.2 *M* Lithium Sulfate	0.1 *M* Tris HCl pH 8.5	30% *v/v* PEG 4000	15% *v/v*	5% *v/v*	5% *v/v*	5% *v/v*
18	0.2 *M* Magnesium Acetate	0.1 *M* Na Cacodylate pH 6.5	20% *v/v* PEG 8000	20% *v/v*	15% *v/v*	20% *v/v*	10% *v/v*
19	0.2 *M* Ammonium Acetate	0.1 *M* Tris HCl pH 8.5	30% *v/v* Isopropanol	20% *v/v*	25% *v/v*	25% *v/v*	20% *v/v*
20	0.2 *M* Ammonium Sulfate	0.1 *M* Na Acetate pH 4.6	25% *w/v* PEG 4000	20% *v/v*	15% *v/v*	15% *v/v*	10% *v/v*
21	0.2 *M* Magnesium Acetate	0.1 *M* Na Cacodylate pH 6.5	30% *v/v* MPD	None	None	None	None
22	0.2 *M* Na Acetate	0.1 *M* Tris HCl pH 8.5	30% *w/v* PEG 4000	15% *v/v*	10% *v/v*	10% *v/v*	5% *v/v*
23	0.2 *M* Magnesium Chloride	0.1 *M* Na HEPES pH 7.5	30% *v/v* PEG 400	None	None	None	None
24	0.2 *M* Calcium Chloride	0.1 *M* Na Acetate pH 4.6	20% *v/v* Isopropanol	30% *v/v*	30% *v/v*	30% *v/v*	20% *v/v*
25	None	0.1 *M* Imidazole pH 6.5	1.0 *M* Na Acetate	30% *v/v*	25% *v/v*	25% *v/v*	20% *v/v*
26	0.2 *M* Ammonium Acetate	0.1 *M* Na Citrate pH 5.6	30% *v/v* MPD	None	None	None	None
27	0.2 *M* Na Citrate	0.1 *M* Na HEPES pH 7.5	20% *v/v* Isopropanol	30% *v/v*	25% *v/v*	25% *v/v*	20% *v/v*
28	0.2 *M* Na Acetate	0.1 *M* Na Cacodylate pH 6.5	30% *w/v* PEG 8000	15% *v/v*	5% *v/v*	10% *v/v*	5% *v/v*
29	None	0.1 *M* Na HEPES pH 7.5	0.8 *M* Potassium Na Tartrate	35% *v/v*	30% *v/v*	30% *v/v*	30% *v/v*
30	0.2 *M* Ammonium Sulfate	None	30% *w/v* PEG 8000	15% *v/v*	10% *v/v*	15% *v/v*	5% *v/v*
31	0.2 *M* Ammonium Sulfate	None	30% *v/v* PEG 4000	15% *v/v*	10% *v/v*	10% *v/v*	5% *v/v*
32	None	None	2.0 *M* Ammonium Sulfate	25% *v/v*	Emulsion (15%)	25% *v/v*	20% *v/v*
33	None	None	4.0 *M* Na Formate	**10% *v/v***	5% *v/v*	10% *v/v*	10% *v/v*
34	None	0.1 *M* Na Acetate pH 4.6	2.0 *M* Na Formate	30% *v/v*	20% *v/v*	25% *v/v*	20% *v/v*
35	None	0.1 *M* Na HEPES pH 7.5	0.8 *M* Mono-Na Phosphate 0.8 *M* Mono-K Phosphate	25% *v/v*	Emulsion (30%)	25% *v/v*	20% *v/v*
36	None	0.1 *M* Tris HCl pH 8.5	8% *w/v* PEG 8000	**35% *v/v***	30% *v/v*	30% *v/v*	30% *v/v*
37	None	0.1 *M* Na Acetate pH 4.6	8% *v/v* PEG 4000	30% *v/v*	30% *v/v*	35% *v/v*	20% *v/v*
38	None	0.1 *M* Na HEPES pH 7.5	1.4 *M* Na Citrate	**10% *v/v***	Emulsion (15%)	10% *v/v*	5% *v/v*
39	None	0.1 *M* Na HEPES pH 7.5	2% *v/v* PEG 400, 2.0 *M* Ammonium Sulfate	15% *v/v*	Emulsion (15%)	30% *v/v*	15% *v/v*
40	None	0.1 *M* Na Citrate pH 5.6	20% *v/v* Isopropanol, 20% *w/v* PEG 4000	5% *v/v*	10% *v/v*	10% *v/v*	10% *v/v*
41	None	0.1 *M* Na HEPES pH 7.5	10% *v/v* Isopropanol, 20% *w/v* PEG 4000	15% *v/v*	15% *v/v*	20% *v/v*	15% *v/v*
42	0.05 Mono-K Phosphate	None	20% *w/v* PEG 8000	20% *v/v*	20% *v/v*	25% *v/v*	20% *v/v*
43	None	None	30% *w/v* PEG 1500	20% *v/v*	10% *v/v*	15% *v/v*	10% *v/v*
44	None	None	0.2 *M* Magnesium Formate	50% *v/v*	35% *v/v*	30% *v/v*	30% *v/v*
45	0.2 *M* Zinc Acetate	0.1 *M* Na Cacodylate pH 6.5	18% *w/v* PEG 8000	20% *v/v*	15% *v/v*	20% *v/v*	10% *v/v*
46	0.2 *M* Calcium Acetate	0.1 *M* Na Cacodylate pH 6.5	18% *w/v* PEG 8000	20% *v/v*	25% *v/v*	20% *v/v*	20% *v/v*
47	None	0.1 *M* Na Acetate pH 4.6	2.0 *M* Ammonium Sulfate	20% *v/v*	Emulsion (25%)	25% *v/v*	20% *v/v*
48	None	0.1 *M* Tris HCl pH 8.5	2.0 *M* Ammonium Phosphate	**20% *v/v***	Crystals (35%)	25% *v/v*	20% *v/v*
49	1.0 *M* Lithium Sulfate	None	2% *w/v* PEG 8000	20% *v/v*	20% *v/v*	25% *v/v*	15% *v/v*
50	0.5 *M* Lithium Sulfate	None	15% *w/v* PEG 8000	20% *v/v*	15% *v/v*	25% *v/v*	10% *v/v*

(*b*) Hampton Screen II

#	Salt	Buffer	Precipitant	Glycerol	PEG 400	EG	PG
1	2.0 *M* Sodium Chloride	None	10% *w/v* PEG 6000	20% *v/v*	20% *v/v*	20% *v/v*	15% *v/v*
2	0.01 *M* CTAB	None	0.5 *M* Sodium Chloride, 0.01 *M* Magnesium Chloride	40% *v/v*	35% *v/v*	35% *v/v*	25% *v/v*
3	None	None	25% *v/v* Ethylene Glycol	15% *v/v*	10% *v/v*	10% *v/v*	5% *v/v*
4	None	None	35% *v/v* Dioxane	25% *v/v*	25% *v/v*	20% *v/v*	15% *v/v*

Table 2 (continued)

#	Salt	Buffer	Precipitant	Glycerol	PEG 400	EG	PG
5	2.0 *M* Ammonium Sulfate	None	5% *v/v* Isopropanol	25% *v/v*	Emulsion (25%)	25% *v/v*	20% *v/v*
6	None	None	1.0 *M* Imidazole pH 7.0	35% *v/v*	30% *v/v*	35% *v/v*	25% *v/v*
7	None	None	10% *w/v* PEG 1000, 10% *w/v* PEG 8000	20% *v/v*	20% *v/v*	20% *v/v*	15% *v/v*
8	1.5 *M* Sodium Chloride	None	10% *v/v* Ethanol	30% *v/v*	25% *v/v*	25% *v/v*	20% *v/v*
9	None	0.1 *M* Na Acetate pH 4.6	2.0 *M* Sodium Chloride	25% *v/v*	20% *v/v*	25% *v/v*	20% *v/v*
10	0.2 *M* Sodium Chloride	0.1 *M* Na Acetate pH 4.6	30% *v/v* MPD	None	None	None	None
11	0.01 *M* Cobalt Chloride	0.1 *M* Na Acetate pH 4.6	1.0 *M* 1,6 Hexanediol	20% *v/v*	25% *v/v*	25% *v/v*	20% *v/v*
12	0.1 *M* Cadmium Chloride	0.1 *M* Na Acetate pH 4.6	30% *v/v* PEG 400	5% *v/v*	5% *v/v*	10% *v/v*	5% *v/v*
13	0.2 *M* Ammonium Sulfate	0.1 *M* Na Acetate pH 4.6	30% *w/v* PEG MME 2000	10% *v/v*	10% *v/v*	10% *v/v*	10% *v/v*
14	0.2 *M* K/Na Tartrate	0.1 *M* Na Citrate pH 5.6	2.0 *M* Ammonium Sulfate	25% *v/v*	Emulsion (10%)	25% *v/v*	15% *v/v*
15	0.5 *M* Ammonium Sulfate	0.1 *M* Na Citrate pH 5.6	1.0 *M* Lithium Sulfate	25% *v/v*	Emulsion (25%)	25% *v/v*	20% *v/v*
16	0.5 *M* Sodium Chloride	0.1 *M* Na Citrate pH 5.6	2% *w/v* Ethylene Imine Polymer	40% *v/v*	Emulsion (20%)	35% *v/v*	25% *v/v*
17	None	0.1 *M* Na Citrate pH 5.6	35% *v/v tert*-Butanol	20% *v/v*	25% *v/v*	15% *v/v*	15% *v/v*
18	0.01 *M* Ferric Chloride	0.1 *M* Na Citrate pH 5.6	10% *v/v* Jeffamine M-600	30% *v/v*	25% *v/v*	35% *v/v*	20% *v/v*
19	None	0.1 *M* Na Citrate pH 5.6	1.0 *M* 1,6 Hexanediol	5% *v/v*	5% *v/v*	5% *v/v*	10% *v/v*
20	None	0.1 *M* MES pH 6.5	1.6 m Magnesium Sulfate	20% *v/v*	15% *v/v*	20% *v/v*	10% *v/v*
21	0.2 *M* Na/K Phosphate	0.1 *M* MES pH 6.5	2.0 *M* Sodium Chloride	25% *v/v*	25% *v/v*	25% *v/v*	20% *v/v*
22	None	0.1 *M* MES pH 6.5	12% *w/v* PEG 20,000	35% *v/v*	25% *v/v*	30% *v/v*	25% *v/v*
23	1.6 *M* Ammonium Sulfate	0.1 *M* MES pH 6.5	10% *v/v* Dioxane	25% *v/v*	Emulsion (15%)	20% *v/v*	15% *v/v*
24	0.05 *M* Caesium Chloride	0.1 *M* MES pH 6.5	30% *v/v* Jeffamine M-600	None	None	None	None
25	0.01 *M* Cobaltous Chloride	0.1 *M* MES pH 6.5	1.8 *M* Ammonium Sulfate	25% *v/v*	Emulsion (20%)	25% *v/v*	20% *v/v*
26	0.2 *M* Ammonium Sulfate	0.1 *M* MES pH 6.5	30% *w/v* PEG MME 5000	10% *v/v*	10% *v/v*	10% *v/v*	10% *v/v*
27	0.01 *M* Zinc Sulfate	0.1 *M* MES pH 6.5	25% *w/v* PEG MME 550	10% *v/v*	10% *v/v*	10% *v/v*	10% *v/v*
28	None	None	1.6 *M* Sodium Citrate pH 6.5	None	None	None	None
29	0.5 *M* Ammonium Sulfate	0.1 *M* HEPES pH 7.5	30% *v/v* MPD	None	None	None	None
30	None	0.1 *M* HEPES pH 7.5	10% *w/v* PEG 6000, 5% *v/v* MPD	20% *v/v*	25% *v/v*	25% *v/v*	15% *v/v*
31	None	0.1 *M* HEPES pH 7.5	20% *v/v* Jeffamine M-600	15% *v/v*	10% *v/v*	15% *v/v*	10% *v/v*
32	0.1 *M* Sodium Chloride	0.1 *M* HEPES pH 7.5	1.6 *M* Ammonium Sulfate	25% *v/v*	Emulsion (25%)	25% *v/v*	20% *v/v*
33	None	0.1 *M* HEPES pH 7.5	2.0 *M* Ammonium Formate	30% *v/v*	30% *v/v*	30% *v/v*	25% *v/v*
34	0.05 *M* Cadmium Sulfate	0.1 *M* HEPES pH 7.5	1.0 *M* Na Acetate	25% *v/v*	25% *v/v*	30% *v/v*	20% *v/v*
35	None	0.1 *M* HEPES pH 7.5	70% *v/v* MPD	None	None	None	None
36	None	0.1 *M* HEPES pH 7.5	4.3 *M* Sodium Chloride	15% *v/v*	10% *v/v*	10% *v/v*	10% *v/v*
37	None	0.1 *M* HEPES pH 7.5	10% *w/v* PEG 8000, 8% *v/v* Ethylene Glycol	25% *v/v*	20% *v/v*	25% *v/v*	15% *v/v*
38	None	0.1 *M* HEPES pH 7.5	20% *w/v* PEG 10000	25% *v/v*	25% *v/v*	20% *v/v*	15% *v/v*
39	0.2 *M* Magnesiuim Chloride	0.1 *M* TRIS pH 8.5	3.4 *M* 1,6 Hexanediol	None	None	None	None
40	None	0.1 *M* TRIS pH 8.5	25% *v/v tert*-Butanol	25% *v/v*	25% *v/v*	30% *v/v*	20% *v/v*
41	0.01 *M* Nickel (II) Chloride	0.1 *M* TRIS pH 8.5	1.0 *M* Lithium Sulfate	25% *v/v*	20% *v/v*	25% *v/v*	15% *v/v*
42	1.5 *M* Ammonium Sulfate	0.1 *M* TRIS pH 8.5	12% *v/v* Glycerol	15% *v/v*	15% *v/v*	20% *v/v*	10% *v/v*
43	0.2 *M* Ammonium Phosphate	0.1 *M* TRIS pH 8.5	50% *v/v* MPD	None	None	None	None
44	None	0.1 *M* TRIS pH 8.5	20% *v/v* Ethanol	25% *v/v*	30% *v/v*	35% *v/v*	20% *v/v*
45	0.01 *M* Nickel (II) Chloride	0.1 *M* TRIS pH 8.5	20% *w/v* PEG MME 2000	20% *v/v*	20% *v/v*	20% *v/v*	15% *v/v*
46	0.1 *M* Sodium Chloride	0.1 *M* Bicine pH 9.0	20% *w/v* PEG MME 550	15% *v/v*	15% *v/v*	15% *v/v*	15% *v/v*
47	None	0.1 *M* Bicine pH 9.0	2.0 *M* Magnesium Chloride	5% *v/v*	5% *v/v*	5% *v/v*	5% *v/v*
48	2% *v/v* Dioxane	0.1 *M* Bicine pH 9.0	10% *w/v* PEG 20000	30% *v/v*	30% *v/v*	30% *v/v*	20% *v/v*

Table 3
Summary of X-ray data processing for a cryocooled lysozyme crystal, space group $P4_32_12$, at 100 K and as the crystal was warmed at rate of 1 K min^{-1}, equating to 1 K per image.

The numbers in parentheses are for the highest resolution shell, 2.18 to 2.10 Å.

	100 K data	Warm up
Number of images	64	64
ΔT (K)	0	64
Cell parameters, $a = b$, c (Å)	78.09, 36.93	78.19, 37.00
Mosaicity (°)	0.48	0.47
Completeness to 2.1 Å (%)	98.6 (99.9)	97.5 (93.7)
R factor (%)	6.6 (21.0)	7.3 (30.7)
$I/\sigma(I)$	21.1 (7.8)	20.8 (4.0)

propyleneglycol with similar molecular weight to PEG 400. It is observed that as the concentration of Jeffamine M-600 decreases, the necessary concentration of cryoprotectant increases (II-18 and II-31). Another observation of note is that 3.4 *M* 1,6-hexanediol (II-39) requires no additional cryoprotectant, 2.5 *M* 1,6-hexanediol (II-19) requires minimal cryoprotectant and 1.0 *M* 1,6-hexanediol (II-11) requires a moderate amount of cryoprotectant. Thus, the amount of cryoprotectant needed follows a predictable pattern and a critical concentration of 1,6-hexanediol required for successful cryocooling exists between 3.4 and 2.5 *M*. Another observation of Mitchell & Garman (1996) confirmed here is that the higher molecular weight PEGs do not seem to provide efficient cryoprotectant themselves; however, when present at higher concentrations, lower concentrations of cryoprotectant are necessary to preserve those conditions.

For PEG 400 in both Hampton Screens, I and II, 96% of the conditions identified visually as a success required the same (37%) or less (59%) cryoprotectant as determined by the X-ray data. For ethylene glycol in both Hampton Screens, 87% of the conditions identified visually as a success required the

same (33%) or less (54%) cryoprotectant as determined by the X-ray data. For glycerol in Hampton Screen II, 73% of the conditions identified visually as a success required the same (56%) or less (17%) cryoprotectant as determined by the X-ray data. In general, visual observation of clear amorphous glass formation is a good indicator of the resulting success of the cryoprotectant conditions for X-ray analysis. However, confirmation by X-ray analysis should always be performed, especially when using glycerol as a cryoprotectant, to ensure that the cryoprotectant solution does not form crystallites that are visually undetectable. For Hampton Screen I, (2*R*,3*R*)-(−)-2,3-butanediol was used in conditions 2, 3, 29, 36 and 44, and was required at concentrations of 25, 25, 20, 25 and 20%, respectively, to form an amorphous glass successfully. For Hampton Screen II, (2*R*, 3*R*)-(−)-2,3-butanediol was used in conditions 2, 6, 16 and 22, and was required at concentrations of 25, 20, 20 and 20%, respectively, for successful cryoprotection.

Fig. 4 shows the cryoprotectant quality number plotted against cryoprotectant concentration when mixed with a pure water solution. There is a minimum reached for each cryoprotectant and beyond this minimum the cryoprotectant itself starts contributing to the X-ray scatter. The minimum is fairly broad, showing that in the case of the cryoprotectants used, a 5% sampling step is adequate for locating initial cryoprotectant conditions. Note that in the case of 1,2-propanediol, the cryoprotection quality index with pure water and increasing concentrations of cryoprotectant did not drop below 1.5.

The structural data for the cryocooled then subsequently warmed lysozyme crystal are summarized in Table 3. It was not obvious from visual examination of the images that ice formation was occurring, but it was clear that the diffraction from the crystal was degrading with temperature in comparison with the same images recorded at 100 K. This was very clear in the data processing, with a rise in scale factor associated with temperature. After applying our analysis technique with a blank loop as a reference, there was no trend in the standard deviation of the data showing any warming effects. The technique, in its current form, was unable to flag potential developing problems in data collection. More severe problems, such as loss of the outer cooling stream, could be picked up, but again conventional data processing is more suited to flagging these. Our method, as presented, is more suitable for quantification of cryoprotectant conditions than as a diagnostic during data collection.

4. Discussion and concluding remarks

In this case, the visual observation of the drop of solution upon flash cooling gives a good initial indication of the success of the cryoprotectant for X-ray data collection. Good illumination of the sample may not always be available *in situ* and taking X-ray data is always recommended. However, examining the X-ray data by eye can be subjective in determining better cryoprotectant conditions. The method of assigning a cryoprotection quality index described here was over 90% accurate in identifying successful cryoconditions. Of the cases where a clear glass was formed, but the cryoprotection quality number was above 1.5, nearly all can be explained. Most of these false negative conditions were never more than 0.2 greater than 1.5 and had a high percentage of cryoprotectant. Thus, it is possible that the increased percentage of cryoprotectant provided more density for X-ray scatter, increasing the slope of the intensity curve in the 'signal' range. False positive results were less obvious in their pattern of failure. Upon examining the raw X-ray images, undesirable dark rings were plainly visible; however, in most cases these ice rings seemed more diffuse than the rings observed in cases where ice rings did not escape detection. These diffuse ice rings did not exhibit a sharp increase in intensity with a sharp decline at higher resolution; rather there was a more gradual rise and fall in intensity over the resolution range where the rings occurred, with similar profiles on the high- and low-resolution sides. Because of this more gradual slope of the intensity *versus* resolution curve, these conditions would have escaped detection by our criterion based on the rate of change of intensity *versus* resolution. The intensity of these rings was still high compared with conditions that exhibited only background diffuse scattering, so it may be possible to determine empirically an upper limit of intensity in the 'signal' range to distinguish these conditions with more diffuse ice rings from conditions with low-level diffuse scattering from a clear solution.

There are limitations in our use of this analysis technique. We have only looked at one loop size, cryogen flow rate, angle of incidence of cryogen on the loop, and distance of cryostat nozzle from the loop. Cryocooling occurs in a wave through the sample being cooled (Snell *et al.*, 2002). This wave travels at a finite speed and so cryoconditions established for a large loop will also apply to smaller ones. The flow rate of the cryostream, 0.44 ms^{-1}, is standard for this apparatus and far faster than the speed of the cold wave through the crystal. It would seem that an increase in flow rate would have marginal effects on the cooling. The angle of incidence will only affect the cooling properties through aerodynamic interference. Our setup was positioned such that the flow was laminar without disruption from the goniometer. Experimental setups in which the flow is directed past the sample down the rotation axis of the goniometer, *e.g.* beamlines at Stanford Synchrotron Radiation Laboratory, work well. The angle of incidence of the stream seems to have marginal if any effect on the cooling. The temperature of the coldstream increases as a function of distance from the tip. In practice, this increase is marginal over the distance used (less than 1 K).

Of perhaps somewhat more importance, we have not examined different methods of cooling. Teng & Moffat (1998) examined cooling with gaseous nitrogen and helium, and plunging into liquid nitrogen and propane. Cooling rates varied with the cryogen and sample size, with larger samples taking longer to cool. The method developed here is equally applicable to studying the effect of the cooling method as well as finding optimum cryoprotectant concentrations. Practically, we find little difference in results with cooling by plunging in

liquid nitrogen *versus* direct gas cooling in the cryostream. We have not explored propane or helium cooling.

In choosing glycerol, PEG400, ethylene glycol, 1,2-propanediol, (2*R*,3*R*)-(−)-2,3-butanediol, MPD and xylitol, we tried to sample a variety of cryoprotectant types. Glycerol is often used but is not always the optimal choice. Some cryoprotectants may adversely affect the stability of the crystal in the cryoprotectant solution. Different cryoprotectants can interact differently with the protein by altering the folding, interfering with crystal contacts, changing enzymatic activity, and interfering with ligand or cofactor binding (Tsitsanou *et al.*, 1999).

The search for an ideal cryosolution can be almost as challenging as determination of the initial crystallization conditions. MPD and xylitol may be impractical for general use as additive cryoprotectants, given the high concentrations required. However, their use should not be ruled out. Samples may be grown using these in the initial conditions and we have not explored combinational effects of different cryoprotectants. This study reports the minimum amount of cryoprotectant to prevent crystalline ice rings seen in the X-ray data. This minimum can be further reduced if the protein sample itself is present in the cryoprotectant solution (Sartor *et al.*, 1995). The crystal may have unforeseen effects on the formation of ice crystals in the cryosolution and may alter the percentage of cryoprotectant necessary to form an amorphous glass. The results presented here are not final cryoprotectant conditions but offer several starting points for the cryoprotectant search and optimization. Optimizing the conditions, by increasing cryoprotectant above the minimum concentration needed to suppress ice formation, is an important step, which can decrease the mosaicity and increase the diffraction limit (Mitchell & Garman, 1994). Our method allows us to quantify the conditions, rapidly opening up systematic studies of cryoprotectants to enhance cryogenic preservation during structural data collection.

MBM and EHS are contracted to NASA through USRA. This work was funded by a NASA NRA award NAG8-1836. Dr Mark van der Woerd is thanked for useful discussions. David Donovan (MSFC) is thanked for technical support.

References

Angell, C. A. & Choi, Y. (1986). *J. Microsc.* **141**, 251–261.
Cosier, J. & Glazer, M. (1986). *J. Appl. Cryst.* **19**, 105–107.
Echlin, P. (1992). *Low-Temperature Microscopy and Analysis.* New York: Plenum Press.
Garman, E. (1999). *Acta Cryst.* D**55**, 1641–1653.
Garman, E. F. & Mitchell, E. P. (1996). *J. Appl. Cryst.* **29**, 584–587.
Garman, E. F. & Schneider, T. R. (1997). *J. Appl. Cryst.* **30**, 211–237.
Jancarik, J. & Kim, S.-H. (1991). *J. Appl. Cryst.* **24**, 409–411.
Mitchell, E. P. & Garman, E. F. (1994). *J. Appl. Cryst.* **27**, 1070–1074.
Otwinowski, Z. & Minor, W. (1997). *Processing of X-ray Diffraction Data Collected in Oscillation Mode*, in *Methods in Enzymology*, edited by R. M. Sweet & C. W. J. Carter. New York: Academic Press.
Rodgers, D. W. (1994). *Structure*, **2**, 1135–40.
Rodgers, D. W. (1997). *Practical Cryocrystallography*, in *Macromolecular Crystallography Part B*, edited by C. W. J. Carter & R. M. Sweet. New York: Academic Press.
Sartor, G., Hallbrucker, A. & Mayer, E. (1995). *Biophys. J.* **69**, 2679–94.
Snell, E. H., Judge, R. A., Larson, M. & van der Woerd, M. J. (2002). *J. Synchrotron Rad.* In the press.
Steinbrecht, R. A. & Zierold, K. (1987). *Cryotechniques in Biological Electron Microscopy.* Berlin: Springer-Verlag.
Teng, T. Y. & Moffat, K. (1998). *J. Appl. Cryst.* **31**, 252–257.
Tsitsanou, K. E., Oikonomakos, N. G., Zographos, S. E., Skamnaki, V. T., Gregoriou, M., Watson, K. A., Johnson, L. N. & Fleet, G. W. (1999). *Protein Sci.* **8**, 741–749.